

cannot be ruled out completely, plausibility arguments disfavor this explanation. For instance, it seems improbable indeed that inhomogeneity broadening would lead always to a linear dependence of R_{\square}' on T (for $0 \lesssim \tau \lesssim 0.2$). Equally inexplicable, in terms of a sample inhomogeneity explanation, is the result that the data points for the 18 samples in the τ_0 -versus- R_{\square}^n plot (Fig. 2) all fall close to a smooth curve, in view of the fact that the samples vary widely in terms of the method of preparation and sample characteristics. In addition, our results on clean aluminum films have been corroborated in at least two other laboratories.^{24,25} Finally, it has been found that samples with $R_{\square}^n \gtrsim 100 \Omega/\text{square}$ yield results which agree with Marčelja's extension of the theory below T_c but do not agree with the AL theory above T_c .

²⁵ M. A. Kleinin and M. A. Jensen (private communication).

Note added in proof. Thompson²⁰ predicts that the excess conductivity σ_a' arising from the Maki term in 2-dim films is given by

$$\sigma_a' = [2\tau_0/(\epsilon + \tau_0)] \ln[(\epsilon + \delta\tau)/\delta\tau],$$

where $\delta\tau$ is the fractional decrease in T_c due to the presence of some pairbreaking perturbation. In the limit of small ϵ , σ_a' should become vanishingly small. An examination of the data close to T_c (e.g., $0 < \epsilon \lesssim 0.01$) for the clean samples used in the present study reveals that this does indeed happen (i.e., $\sigma' \approx \sigma_{AL}'$ in the limit of small ϵ).

ACKNOWLEDGMENTS

It is our pleasure to thank J. E. Crow, S. Marčelja, M. Strongin, and R. Thompson for helpful discussions, and D. Lawrence for his help with data analysis and experimental details.

Thermal-Conductivity Measurements of Gapless Behavior Produced by the Proximity Effect*

G. DEUTSCHER,[†] P. LINDENFELD, AND R. D. MCCONNELL[‡]

Department of Physics, Rutgers University, New Brunswick, New Jersey 08903

(Received 6 October 1969)

The thermal conductivities K_s and K_n in the superconducting and normal states have been measured for six In-Bi films of varying thickness with Mn layers on each side. The graphs of K_s/K_n against T show the characteristic linear variation of gapless systems near the transition temperature. In contrast to the expected behavior, K_s/K_n approaches a finite value at low temperatures. This is interpreted in terms of localized states near the n - s boundary which cause gapless behavior at all temperatures.

I. INTRODUCTION

THE properties of a superconducting film are affected by the proximity of a normal metal in good contact with it, particularly if the normal metal is magnetic.¹ The most obvious effect is the reduction in the transition temperature. In addition both theoretical calculations and tunneling experiments have shown that there are profound changes in the density of states, such that there is no energy gap in the vicinity of the transition temperature. We have made thermal-conductivity experiments which confirm these features and which, in addition, show some unexpected behavior which may be interpreted in terms of localized states

near the boundary which cause a portion of the specimen to remain gapless (or have only a small gap) at all temperatures.²

For a description of our results and a comparison with the theory we consider two different temperature regions. Near the transition temperature the ratio of the superconducting and normal thermal conductivities (K_s/K_n) varies linearly with temperature as for other gapless systems.³ A quantitative comparison of theory and experiment requires that we take into account the spatial variation of the order parameter resulting from the proximity effect, and this is discussed in Secs. II A and V A.

At low temperatures the variation of K_s/K_n gives

* Supported by the National Science Foundation, the Rutgers Research Council, and the U. S. Army Electronics Laboratory, Fort Monmouth, N. J.

[†] Permanent address: Faculté des Sciences, Orsay, France.

[‡] Permanent address: Université de Montréal, Montreal, Canada.

¹ For a review of the subject and a comprehensive list of references see G. Deutscher and P. G. de Gennes, in *Superconductivity*, edited by R. D. Parks (Marcel Dekker, Inc., New York, 1969), Vol. 2, Chap. 17.

² Two preliminary accounts of this work have been published: G. Deutscher, P. Lindenfeld, and R. D. McConnell, *Phys. Rev. Letters* **21**, 79 (1968); and in *Proceedings of the Eleventh International Conference on Low-Temperature Physics, St. Andrews, Scotland, 1968*, edited by J. F. Allen, D. M. Finlayson, and D. M. McCall (University of St. Andrews Printing Dept., St. Andrews, Scotland, 1969), p. 993.

³ K. Maki, Ref. 1, Chap. 18.

direct information on the density of states. In particular, the presence of a gap leads to an exponential decrease of K_s/K_n as absolute zero is approached. It is here that our results depart from the expected behavior by indicating the approach to a finite value of K_s/K_n , and hence the persistence of gaplessness to the lowest temperatures. This is discussed in Secs. II B and V B.

The experimental procedures and the methods of analysis are described in Sec. III and the specimen characteristics in Sec. IV. In Sec. VI we discuss other experiments which shed light on the existence of localized states near the normal-superconducting boundary.

II. THEORY

A. Near T_{cns}

The expected thermal conductivity can be described in detail near the transition temperature. One can use the expression of Caroli and Cyrot⁴ which is valid to order $|\Delta|^2$, together with the Wiedemann-Franz law,

$$R = K_s/K_n = 1 - (3/2\pi^2 k^2 T_{cns}^2) \langle |\Delta|^2 \rangle \times \rho [\psi^{(1)}(\rho + \frac{1}{2}) + \rho \psi^{(2)}(\rho + \frac{1}{2})],$$

where $\rho = Dq^2/4\pi T_{cns}$ and satisfies the equation

$$\ln t_c + \psi(\rho + \frac{1}{2}) - \psi(\frac{1}{2}) = 0.$$

Here, $t_c = T_{cns}/T_{cs}$, where T_{cns} is the transition temperature of the sandwich specimen and T_{cs} the transition temperature of the superconductor alone.

For the spatial average of the order parameter we use the expression of Fulde and Maki⁵ as generalized by Maki³:

$$\langle |\Delta|^2 \rangle = \frac{8\pi^2 T_{cns}^2 [1 - \rho \psi^{(1)}(\rho + \frac{1}{2})] (1 - t)}{\beta_1 [-\frac{1}{2} \psi^{(2)}(\rho + \frac{1}{2}) + (\beta_2 \rho / 6) \psi^{(3)}(\rho + \frac{1}{2})]},$$

where $t = T/T_{cns}$ and $\psi, \psi^{(1)}, \psi^{(2)}, \psi^{(3)}$ are the digamma, trigamma, tetragamma, and pentagamma functions. β_1 and β_2 are the averages introduced by Maki,

$$\beta_1 = \frac{\langle |\Delta|^4 \rangle}{(\langle |\Delta|^2 \rangle)^2},$$

$$1 + \beta_2 = \frac{\langle [(\partial/\partial x)|\Delta(x)|^2]^2 \rangle}{q^2 \langle |\Delta|^4 \rangle}.$$

We assume that $\Delta(x) = \cos qx$ and can then evaluate β_1 and β_2 to get

$$\beta_1 = \frac{3 + 4(\sin a)/a + (\sin 2a)/2a}{2[1 + (\sin a)/a]^2},$$

$$\beta_2 = \frac{1 - 4(\sin a)/a - 5(\sin 2a)/2a}{3 + 4(\sin a)/a + (\sin 2a)/2a},$$

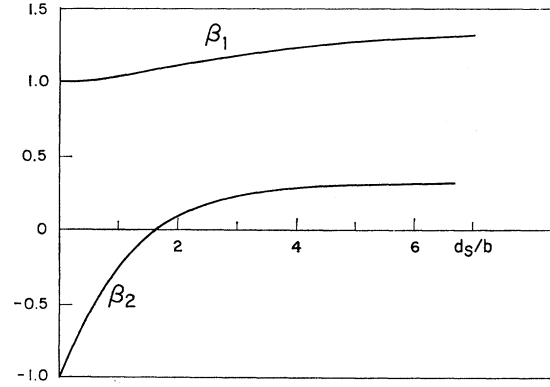


FIG. 1. The parameters β_1 and β_2 as functions of d_s/b .

where $a = 2qd_s$ and $2d_s$ is the film thickness. The expression for β_1 agrees with that given by Maki,³ but his expression for β_2 is in error.

We let $q = \pi/2(d_s + b)$, where b is the extrapolation length¹ defined by

$$\frac{1}{\Delta} \frac{d\Delta}{dx} = -\frac{1}{b}.$$

evaluated at the boundary. We can now write β_1 and β_2 , hence $\langle |\Delta|^2 \rangle$ and K_s/K_n , as functions of d_s/b . The variation of β_1 and β_2 with d_s/b is shown in Fig. 1. The maximum proximity effect corresponds to $b=0$, and this is the case discussed by Fulde and Maki. The values $\beta_1 = \frac{3}{2}$ and $\beta_2 = \frac{1}{3}$ lead to their expression for $\langle |\Delta|^2 \rangle$. When $d_s/b=0$ the order parameter is constant, as for superconductors with paramagnetic impurities. This case has been discussed in detail by Skalski, Betbeder-Matibet, an Weiss,⁶ and by Ambegaokar and Griffin.⁷ In this limit $\beta_1 = 1$ and $\beta_2 = -1$, and with these values their expressions are recovered.

The slope of the graph of K_s/K_n against temperature at $T = T_{cns}$ depends on ρ (hence t_c) and on d_s/b . Figure 2 shows the slope dR/dt as a function of t_c for the two

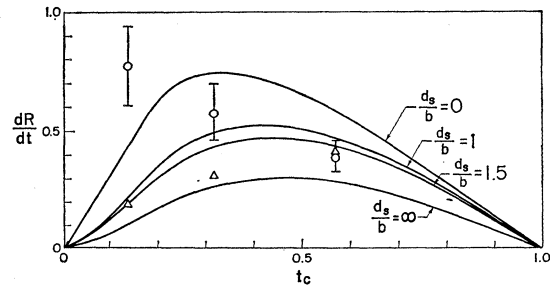


FIG. 2. Theoretical curves of dR/dt against t_c for various values of d_s/b . ($R = K_s/K_n$, $t = T/T_{cns}$, $t_c = T_{cns}/T_{cs}$, $2d_s$ is the thickness of superconductor, b is the extrapolation length.) The circles are the experimental points for specimens 4, 5, and 6. The triangles are the corresponding theoretical values.

⁴ C. Caroli and M. Cyrot, Phys. Kondensierten Materie **4**, 285 (1965).

⁵ P. Fulde and K. Maki, Phys. Kondensierten Materie **5**, 380 (1966).

⁶ S. Skalski, O. Betbeder-Matibet, and P. R. Weiss, Phys. Rev. **136**, A1500 (1964).

⁷ V. Ambegaokar and A. Griffin, Phys. Rev. **137**, 1151 (1965).

limiting values of d_s/b of zero and infinity, as well as for two intermediate values.

For all values of d_s/b the slope is zero at $t_c=1$. This is in accord with the fact that there is then no proximity effect, and the theory of Bardeen, Rickayzen, and Tewordt⁸ (BRT) applies.

The slope also goes to zero as t_c goes to zero. This again is to be expected since the proximity effect is then so strong that the density of states approaches that of the normal state.

B. Near 0°K

At temperatures far from the transition temperature the only detailed calculations are those of Ambegaokar and Griffin⁷ for constant order parameter. For this case the material is gapless near the transition temperature, and remains so down to some lower temperature whose value depends on the strength of the pair breaking mechanism. When the pair breaking mechanism is strong enough, corresponding to a reduction in the transition temperature to $t_c \leq 0.2$, the material will be gapless down to $T=0^\circ\text{K}$.

The calculations of Ambegaokar and Griffin lead to curves of K_s/K_n against temperature which show the finite slope near the transition temperature which was described in Sec. II A, which causes the curves to fall below those for ordinary superconductors. As the temperature is reduced, the curves cross the BRT curve and remain above it down to the lowest temperature. As the temperature approaches zero, K_s/K_n also goes to zero, except in specimens which remain gapless at all temperatures. In fact, a finite value of K_s/K_n at $T=0^\circ\text{K}$ can be taken as an experimental indication of gaplessness down to absolute zero, while the presence of an energy gap would be indicated by an exponential decrease in the thermal conductivity.

We have considered only the electronic contribution to the thermal conductivity. In bulk alloy specimens the lattice conductivity is often significant and may even predominate, but in thin films the scattering to phonons by internal and external boundaries usually causes the lattice conductivity to be negligible. Our own measurements show that there is no detectable lattice conductivity in any of our specimens. (See Sec. V B.)

III. EXPERIMENTAL PROCEDURES

The specimens consisted of films of various thicknesses of indium containing between 1 and 2% bismuth, with layers of manganese on each side. They were evaporated onto nitrogen-cooled glass substrates to which a heater and two thermometers were connected subsequently.

In order to insure homogeneity of the indium-bismuth layers most specimens were made by dropping previously prepared alloy pellets into the boat and evaporating them one by one. This precaution is not essential.

Although the evaporation rates of the two constituents are quite different, interdiffusion is apparently rapid enough to ensure homogeneity.⁹

The indium alloy was evaporated from a 5-mil molybdenum boat. The boat was surrounded by a shield to reduce the heat radiation reaching the substrate, and to protect the boat from stray manganese. The manganese was evaporated from a deep cylindrical tantalum boat so as to concentrate the evaporating material in the upward direction.

The substrates were No. 00 microscope cover glass, approximately 1.0 cm wide, 0.007 cm thick, and 2.0 cm long. One end was cemented with GE 7031 varnish to a piece of copper which was later clamped into the cryostat's specimen holder. In the evaporator the substrate was cooled by a copper block strapped to the nitrogen cooling coils. A small drop of glycerin which was later washed off provided the thermal contact between the glass and the copper block.

The pressure was about 5×10^{-7} Torr before and 10^{-6} Torr during the evaporation. The thickness was monitored by a Sloan quartz crystal gauge. For all specimens except for No. 1 the time between the evaporation of successive layers was kept to about seven seconds to prevent the build-up of an oxide layer which would reduce the proximity effect. This was done by keeping the manganese boat hot and letting the manganese evaporate onto a shutter during the evaporation of the indium alloy layer.

For specimen No. 1 the time interval between the evaporation of the layers was about 1 min. Nevertheless there is no evidence that an insulating barrier was present even in that case.

Small amounts of manganese can dissolve in indium causing shifts in T_c up to 0.3°K .¹⁰ In order to retain the manganese in solution the alloy must be quenched and is in any case quite unstable at room temperature. We consider it unlikely that our results were affected by alloying of the manganese.

The thermometers were $\frac{1}{8}$ -W Allen-Bradley resistors. The covering was removed from one side and they were cemented to the back side of the substrate with GE 7031 varnish. The distance between the thermometers was about 0.5 cm. We assumed the effective length of the specimen to be the average of the distance between the inner edges and the distance between the thermometer centers, and the uncertainty to be one-fourth the width of a thermometer, or ± 0.08 cm. The length and width were measured with a cathetometer to ± 0.005 cm.

A constantan heater was cemented to the end of the specimen. The heat power Q developed in it was determined by measuring the current and the voltage with a potentiometer, using three leads to the heater.¹¹

⁹ G. Deutscher, J. Phys. Chem. Solids **28**, 741 (1967).

¹⁰ G. Boato, G. Gallinaro, and C. Rizzuto, Phys. Rev. **148**, 353 (1966).

¹¹ J. F. Cochran, C. A. Shiffman, and J. E. Neighbor, Rev. Sci. Instr. **37**, 499 (1966).

⁸ J. Bardeen, G. Rickayzen, and L. Tewordt, Phys. Rev. **113**, 982 (1959).

The resistances of the thermometers were measured with a Wheatstone bridge circuit. A modified Clement-Quinell equation of the form

$$\frac{1}{T^*} = A \ln R + \frac{B}{\ln R + D} + C$$

was used, and found to fit the calibration points to ± 1 mdeg.¹¹ A germanium thermometer, previously calibrated against the helium vapor pressure, was used as a secondary standard.

After the thermal-conductivity measurements were completed, copper leads were attached to the specimen for measurements of the resistance at 4.2°K and at room temperature. The residual resistivity ρ_s was calculated from the ratio of the two measured resistances and Matthiessen's rule, $\rho(T) = \rho_s + \rho_p(T)$, where $\rho_p(T)$ is the resistivity of pure indium at room temperature, and is given by $7.9/[1 - \beta(T - 273)] \mu\Omega \text{ cm}$, with $\beta = 0.0047 \text{ deg}^{-1}$.^{12,13}

The transition temperature was determined either from the resistance transition, the variation of H_{c2} with T , or by a combination of these methods.

The specimen thicknesses were measured with the Sloan quartz crystal monitor which was calibrated by a series of resistance measurements. They were in good agreement with the measurements of an optical interferometer. We estimate the uncertainty in the specimen thickness to be $\pm 100 \text{ \AA}$.

The quantities which are measured directly in the thermal measurements are the total conductances $Q/\Delta T_n = C_n + C_b$ and $Q/\Delta T_s = C_s + C_b$, and hence the difference $\Delta C = C_n - C_s$, where $C_n = K_n A/L$ and $C_s = K A/L$ are the specimen conductances in the normal and superconducting states, C_b is the background conductance of the substrate, A the cross section, and L the effective length of the specimen. For the thickest specimen (No. 1), C_b was measured in a separate run and subtracted from the measured conductances to get C_s and C_n and hence K_s/K_n . For the other specimens we used the Wiedemann-Franz law, $K_n = L_0 T/\rho_0$, to find C_n , and combined it with ΔC to find C_s .

The temperatures are known to about ± 2 mdeg. The temperature difference ΔT across the specimen was usually between 50 and 100 mdeg. The precision of ΔT depends on the sensitivity of the thermometers and varies with the temperature. At the lowest temperatures changes of a few μdeg can be measured.

The main uncertainty in K_s/K_n when the Wiedemann-Franz law is used comes from the effective length for the thermal measurement. We estimate that C_n , hence ΔC , and $1 - K_s/K_n$ are then known to about 15%.

IV. SPECIMEN CHARACTERISTICS

Specimens 1, 2, 3, and 3A were films of indium alloy with 100 \AA of manganese on each side. In order to increase the specimen conductance relative to that of the substrate the thinner specimens, Nos. 4, 5, and 6, were made as double films, $\text{Mn}|\text{In}|\text{Mn}|\text{In}|\text{Mn}$. The two indium alloy layers had thicknesses within 1% of one another. The central layer of manganese was 200 \AA , the outer layers 100 \AA .

The percentage of bismuth varied somewhat in the different specimens. It may be estimated from the residual resistivity which is about $1.8 \mu\Omega \text{ cm}$ per percent of bismuth.

Specimens 3 and 3A were made in the same evaporation, but only resistivity measurements were made on specimen 3A. The characteristics of all specimens are shown in Table I.

The Ginzburg-Landau parameter κ was determined from the resistivity with the Gor'kov-Goodman relation.¹⁴ (The conductance of the manganese layers was neglected.)

The transition temperature T_{cs} of the indium alloy in the absence of a proximity effect was determined from Fig. 3, which shows κ as a function of T_{cs} from the data of Kinsel, Lynton, and Serin.¹⁵ The figure also shows two points for thin films without manganese, which are seen to be in very good agreement.

The value of the extrapolation length b was determined from the relation¹

$$\frac{1}{\xi(T_{cns})} \tan \frac{d_s}{\xi(T_{cns})} = \frac{1}{b}$$

$\xi(T_{cns})$ was calculated from

$$\xi^2(T_{cns}) = \frac{\phi_0/2\pi}{H_{c2}(T_{cns})}$$

Here $H_{c2}(T_{cns})$ is the upper critical field of the superconductor (without proximity effect) at the temperature T_{cns} . It was determined from the results of Kinsel, Lynton, and Serin, together with the theoretical temperature dependence of H_{c2} .¹⁶

TABLE I. Characteristics of the specimens.

| Sample | d_s \AA | ρ_s $\mu\Omega \text{ cm}$ | $\kappa(T_{cs})$ | T_{cs} (°K) | T_{cns} (°K) | b (\AA) |
|--------|-----------------------|------------------------------------|------------------|------------------|-------------------|-------------------------|
| 1 | 16 000 | 3.04 | 0.83 | 3.81 | 3.75 | 330 |
| 2 | 3250 | 3.62 | 1.006 | 3.91 | 3.00 | 260 |
| 3 | 3060 | (3.58) | ... | ... | 3.03 | ... |
| 3A | 2950 | 3.58 | 0.996 | 3.90 | 2.81 | 260 |
| 4 | 2160 | 2.89 | 0.815 | 3.80 | 2.17 | 590 |
| 5 | 1940 | 3.86 | 1.092 | 3.97 | 1.25 | 240 |
| 6 | 1890 | 2.25 | 0.651 | 3.70 | 0.52 | 610 |

¹⁴ Reference 1, p. 930.

¹⁵ T. Kinsel, E. A. Lynton, and B. Serin, Rev. Mod. Phys. **36**, 105 (1964).

¹⁶ A. L. Fetter and P. C. Hohenberg, Ref. 1, p. 913.

¹² G. K. White and S. B. Woods, Rev. Sci. Instr. **28**, 638 (1957).

¹³ Handbook of Chemistry and Physics (Chemical Rubber Publishing Co., Cleveland, Ohio, 1961), 43rd ed., p. 2634.

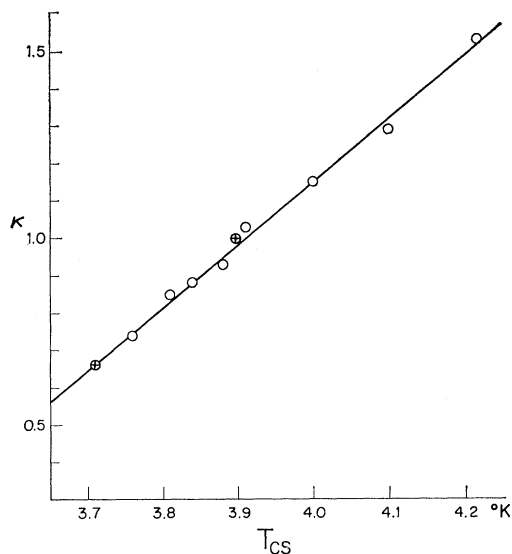


FIG. 3. The Ginzburg-Landau parameter κ as a function of T_{cs} for various indium specimens with bismuth impurity. The open circles are from Ref. 15. The two circles with crosses are for films which were measured to check the validity of the curve.

The extrapolation length can be related to the quantity K^{-1} which is a measure of the distance to which Cooper pairs penetrate into the normal layer¹:

$$b = (\rho_{Mn}/\rho_s)K^{-1},$$

where ρ_{Mn} is the resistivity of the manganese and ρ_s is the residual resistivity of the superconducting layer. Figure 4 shows a graph of b against ρ_s^{-1} . We have measured ρ_{Mn} for a film deposited as on our specimens to be $340 \mu\Omega \text{ cm}$. The value of K^{-1} is then $3.5 \pm 1 \text{ \AA}$. In an antiferromagnetic material the length K^{-1} is primarily a function of the lattice disorder. The fact that K^{-1} is approximately the same for all our specimens therefore tells us that our method of sample preparation is reproducible and consistent.

The only other estimate of K^{-1} in a magnetic material is that of Hauser, Theuerer, and Werthamer¹⁷ for iron in contact with lead, deposited on nitrogen-cooled substrates. Their value for K^{-1} is 6 \AA .

V. RESULTS AND DISCUSSION

A. Near T_{cs}

Figure 5 shows the thermal conductance of specimen No. 1 after subtraction of the measured glass conductance. The normal state conductance divided by the temperature is constant to one percent in accordance with the Wiedemann-Franz law. Figures 6-8 show the curves of K_s/K_n against t for all specimens.

We first consider the region near T_{cs} where the experimental curves have a finite slope as expected from the

¹⁷ J. J. Hauser, H. C. Theuerer, and N. R. Werthamer, Phys. Rev. **142**, 118 (1966).

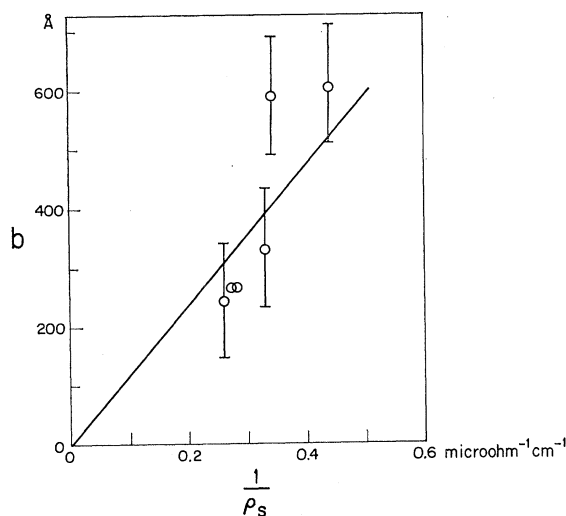


FIG. 4. The extrapolation length b as a function of $1/\rho_s$. ρ_s is the residual resistivity of the specimens.

theory (Sec. II A) and in contrast to the BRT curve which describes the behavior of dilute indium alloys without proximity effect.

Only the three thinnest specimens (Nos. 4, 5, and 6) could be used for a comparison with the theoretical results, because in the thicker ones the region of gaplessness, and therefore the temperature interval in which the theory can be used, is too small. An estimate of the lowest temperature t_g at which the specimen is expected to be gapless can be made with the help of Fig. 4 of Ref. 7. Table II shows the values of t_g for specimens 3, 4, 5, and 6.

Figure 2 shows our results for the slopes, together with the theoretical curves discussed in Sec. II A. It can be seen that for the two thinnest samples the experimental result is higher than that expected from the theory. The result for specimen 5 was checked by measuring the resistivity of a second specimen made in the same evaporation as well as by measuring the substrate conductance after removing the film. The com-

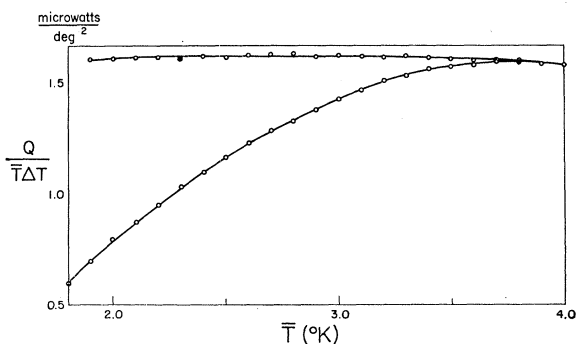


FIG. 5. The conductances divided by the temperature in the normal state (upper curve) and the superconducting state (lower curve) for specimen 1.

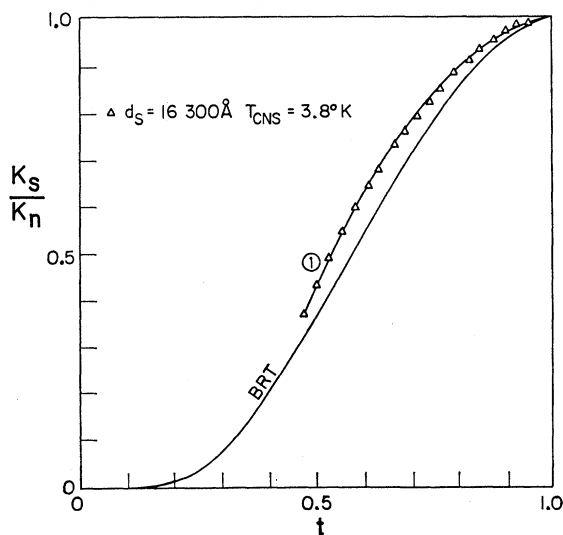


FIG. 6. K_s/K_n for specimen 1. The curve labeled BRT is calculated from Ref. 9 with $2\epsilon_0/kT_c = 3.7$.

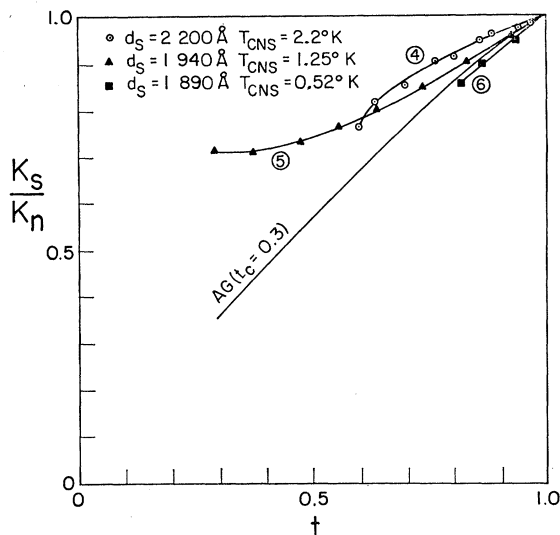


FIG. 8. K_s/K_n for specimens 4, 5, and 6. The curve labeled AG is from Ref. 7 for the same reduced transition temperature as specimen 5.

bination of all measurements gave a slope of 0.63 ± 0.1 , compared with the theoretical value of 0.3.

It is possible that for our thinnest specimens the order parameter no longer varies as a cosine function, so that the parameters β_1 and β_2 are no longer given by the expressions of Sec. II A. It is difficult to see how even then the slopes can be outside the limits of the theoretical curves given by $d_s/b=0$ and $d_s/b=\infty$.

It is quite difficult to prepare specimens with small values of t_c . Very small variations in thickness or impurity concentration will cause the transition temperature to fall below the available temperature range.

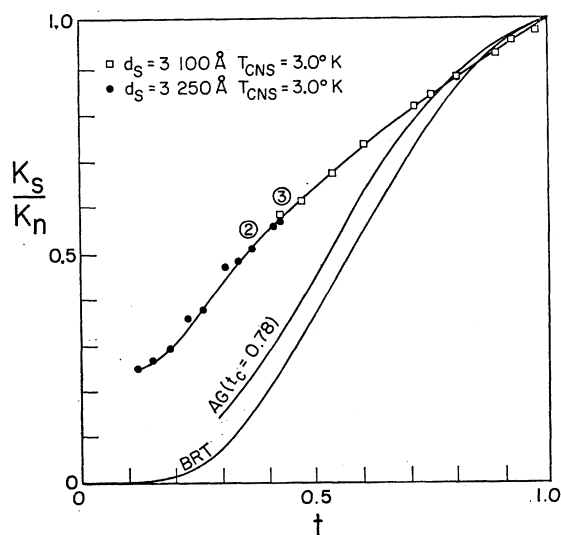


FIG. 7. K_s/K_n for specimens 2 and 3. The curve labeled BRT is the same as in Fig. 6. The curve labeled AG is from Ref. 7 for the same reduced transition temperature as for these specimens.

We did in fact make two runs on a specimen which turned out to be normal down to 0.3°K .

B. Near 0°K

It can be seen from Figs. 6 and 7 that the curves of K_s/K_n against t are, except near T_{cns} , above the BRT curve.

A possibility which must be considered is that there is some lattice conductivity. In bulk specimens of the same composition the lattice component would be quite large and K_s/K_n would lie considerably higher than the BRT curve for the ratio of the electronic components.¹⁸ In thin films scattering by the external boundaries and by lattice defects decreases the lattice conductivity drastically, but in sufficiently thick annealed films there may still be a measurable lattice component. Particularly in the thickest film (No. 1) it cannot be ruled out *a priori* that the difference between the measured K_s/K_n and the BRT curve is the result of lattice conduction.

If this were so, the curves for the other specimens would be expected to approach the BRT curve more and more closely with decreasing thickness. The data show that this is not so. Moreover, the detailed analysis of the curve for specimen No. 1 shows that the deviation of the curve from the BRT curve is entirely consistent with that expected from the proximity effect alone. We therefore assume that lattice conduction plays a negligible role in all our specimens.

Figures 6-8 show that, except near T_{cns} , the experimental curves lie not only above the BRT curve but also above the appropriate curves of Ambegaokar and Griffin⁷ (AG). On Figs. 7 and 8 we show the AG curves

¹⁸ P. Lindenfeld and H. Rohrer, Phys. Rev. **139**, A206 (1965).

TABLE II. Gapless region for specimens 3, 4, 5, and 6 according to Ref. 7.

| Sample | T_{cns} (°K) | T_g (°K) | $t_g = T_g/T_{cns}$ |
|--------|-------------------|---------------|---------------------|
| 3 | 3.03 | 2.97 | 0.98 |
| 4 | 2.17 | 2.01 | 0.93 |
| 5 | 1.25 | 0.84 | 0.67 |
| 6 | 0.52 | 0.00 | 0.00 |

for the same reduced transition temperatures as specimens No. 2, 3, and 5. It can be seen that the deviation is largest at low temperatures, and that it increases with decreasing thickness.

Table II shows that only for the thinnest specimen, No. 6, is the region of gaplessness expected to extend to 0°K with an accompanying finite value of K_s/K_n . The results indicate that K_s/K_n remains finite to 0°K also for specimens 2 and 5.

The main difference between our case and that of AG is that for the proximity effect the order parameter varies rapidly near the boundary over a distance of the order of the coherence length. The situation is reminiscent of that in the vortex cores of type-II superconductors, where a similar variation of the order parameter has been shown to lead to low-lying excited states.¹⁹ We therefore ascribe the finite value of K_s/K_n at low temperatures in our specimens to such states in the region near the boundary.

If we assume that for our experimental situation the localized excitations have the same transport properties as normal electrons, a rough estimate of the expected effect can be made. We consider a region of thickness $\xi(T) - b$ near the boundary to act like a normal metal with the rest behaving like an ordinary superconductor following the BRT curve. With this assumption we can derive the relation $(R - R_B)/(1 - R_B) = 2[\xi(T) - b]/d_s$, where $R = K_s/K_n$ is the ratio of the experimental conductivities and R_B is the value of the ratio of the conductivities calculated according to BRT. This analysis is likely to be useful only when the thickness is sufficiently large compared to the coherence length. We have applied it to specimen 1 by plotting $(R - R_B)/(1 - R_B)$ against the expected temperature dependence of the coherence length, $(1 - T/T_{cs})^{-1/2}$ on Fig. 9. Above $t = 0.7$ the points indeed fall on a straight line, with a slope of 0.09 and an intercept at $t = 0$ of 0.12. The value of the slope corresponds to a coherence length at $T = 0^\circ\text{K}$ of 730 Å, in reasonable agreement with the value 860 Å for a similar specimen according to Kinsell, Lynton, and Serin.¹⁵ The value of the intercept is somewhat more uncertain and corresponds to $\xi(T = 0^\circ\text{K}) - b = 980$ Å.

The assumption of gapless behavior near the boundary is thus qualitatively confirmed. But in our specimens, with their finite extrapolation length, the pair

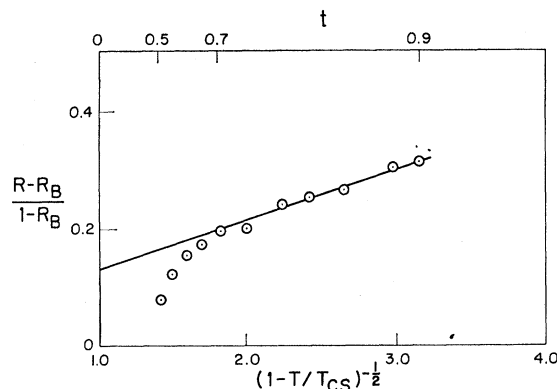


FIG. 9. $R - R_B/1 - R_B$ against $(1 - T/T_{cs})^{-1/2}$ for specimen 1. R is the experimental value and R_B the theoretical value (from Ref. 9) of K_s/K_n .

potential has a finite value at the boundary which for specimens as thick as No. 1 may be identified with the energy gap for the boundary region. Its value can be estimated from the relation²⁰

$$\Delta(d_s) = b\Delta/\xi(T),$$

where 2Δ is the BCS gap. When kT becomes less than $\Delta(d_s)$ we can expect the existence of the gap to dominate the behavior. For specimen No. 1 this should happen in the neighborhood of $t = 0.7$, and we believe that this is the reason for the departure of the experimental points from the straight line on Fig. 9.

For the thinner specimens the separation of the specimen into two regions is no longer appropriate. It may still be possible to estimate the value of K_s/K_n at $T = 0^\circ\text{K}$ by letting R_B go to zero so that $R = 2[\xi(0) - b]/d_s$. We have done this for the two specimens for which we can estimate the value of K_s/K_n at $T = 0^\circ\text{K}$ with some confidence, namely, Nos. 2 and 5. Table III shows the results which are seen to be quite satisfactory.

VI. COMPARISON WITH OTHER EXPERIMENTS

Another confirmation of the existence of localized states comes from some otherwise unexplained tunneling experiments of Hauser²¹ on junctions of

TABLE III. Experimental value of K_s/K_n at $T = 0^\circ\text{K}$, compared with the value estimated by assuming that a region of thickness $\xi(T) - b$ near the boundary has conductivity K_n .

| Sample | t_c | $2[\xi(T = 0) - b]/d_s$ | $(K_s/K_n)_{T=0}$ |
|--------|-------|-------------------------|-------------------|
| 2 | 0.767 | 0.30 ± 0.06 | 0.22 ± 0.01 |
| 5 | 0.315 | 0.51 ± 0.10 | 0.65 ± 0.06 |

¹⁹ C. Caroli and J. Matricon, Phys. Kondensierten Materie **3**, 380 (1965).

²⁰ J. P. Burger, G. Deutscher, J. P. Hurault, and A. Martinet, in *Proceedings of the Tenth International Conference on Low-Temperature Physics, Moscow, 1966*, edited by M. P. Mal'kev (Proizvodstvenno-Izdatel'skii Kombinat VINITI, Moscow, 1967), Vol. 2A, p. 190.

²¹ J. J. Hauser, Phys. Rev. **164**, 558 (1967).

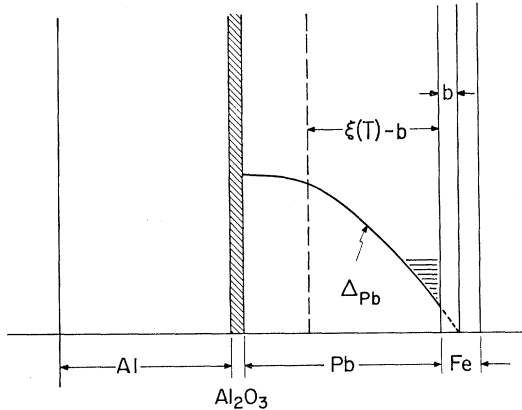


FIG. 10. Schematic behavior of the pair potential for the specimen of Ref. 21.

Al|Al₂O₃|Pb(1300 Å)|Fe (50 Å). Below the transition temperature of aluminum they show the rapid change in dV/dI at zero bias which is characteristic for the absence of a gap in the Pb, while at the same time there is a peak at about 1.2 mV indicating the presence of a gap. In Fig. 10 we sketch the behavior of the pair potential in Hauser's specimen. The low-energy excitations are near the Pb-Fe boundary, but if the distance to the oxide junction is of the order of the coherence length, they may tunnel through the region of high pair potential and give rise to gapless behavior in the tunneling characteristic.

In a film thinner than the coherence length the effect of the gap should disappear completely, and Hauser indeed finds that this is so for a film where the thickness of the Pb is 475 Å.

Microwave measurements on Mn|InBi|Mn specimens have shown that their surface resistance is much larger than that of bare InBi films.²² These results definitely confirm the existence of low-lying states localized near the boundary, because in these specimens (for which $\kappa \gtrsim 1$) the microwave field penetrates only in the boundary region so that the measurements are not affected by the bulk properties of the specimen.

Recent experiments on pure niobium²³ indicate that

²² F. Brochard, G. Deutscher, W. Holzer, P. Pincus, and G. Waysand, in *Proceedings of the International Conference on the Science of Superconductivity*, Stanford University, 1969, paper 12.4 (to be published).

²³ E. M. Forgan, C. E. Gough, M. J. Hood, and W. F. Vinen, in *Proceedings of the Eleventh International Conference on Low-Tem-*

perature Physics, St. Andrews, Scotland, 1968, edited by J. F. Allen, D. M. Finlayson, and D. M. McCall (University of St. Andrews Printing Dept., St. Andrews, Scotland, 1969), p. 934; W. F. Vinen, in *Proceedings of the International Conference on the Science of Superconductivity*, Stanford University, 1969, paper E (to be published).

VII. SUMMARY

The proximity effect has been used to produce samples which display two kinds of gapless behavior with different conceptual aspects.

The gapless behavior as predicted by AG for superconductors with dilute paramagnetic impurities is observed near the critical temperature of the samples, where K_s/K_n is a linear function of the temperature. In this temperature range the spatial variation of the order parameter does not play a major role and can be taken into account by appropriate renormalization factors.

At low temperatures our specimens show a more pronounced gapless behavior than predicted. Even for thick specimens with small shifts of the critical temperature, the experimental values of K_s/K_n lie consistently above those calculated by AG. K_s/K_n values obtained by extrapolation to $T=0^\circ\text{K}$ vary as $1/d_s$, whereas the critical temperature varies approximately as $1/d_s^2$. These results are ascribed to the rapid variation of the pair potential near the proximity effect boundary, which is thought to produce low lying states localized within one coherence length of the boundary.

ACKNOWLEDGMENTS

One of us (G. D.) would like to thank Rutgers University and his colleagues for their hospitality during the course of this research.

perature Physics, St. Andrews, Scotland, 1968, edited by J. F. Allen, D. M. Finlayson, and D. M. McCall (University of St. Andrews Printing Dept., St. Andrews, Scotland, 1969), p. 934; W. F. Vinen, in *Proceedings of the International Conference on the Science of Superconductivity*, Stanford University, 1969, paper E (to be published).